SEMARAK ILMU PUBLISHING

Journal of Advanced Research in Applied Mechanics

Journal homepage:
https://semarakilmu.com.my/journals/index.php/appl_mech/index
ISSN: 2289-7895

Computational Simulation and Experimental Analysis of Activated Carbon from Agricultural Waste as Electromagnetic Absorber

Nawrah Afnan Ashraf[1], Fadzidah Mohd Idris[2,*], Noorain Purhanudin[2], Syahida Suhaimi[1], Intan Helina Hassan[3]

[1] Energy Materials Research Consortium, Faculty of Science and Technology, Universiti Sains Islam Malaysia, 71800, Nilai, Negeri Sembilan, Malaysia
[2] Kolej PERMATA Insan, Universiti Sains Islam Malaysia, 71800, Nilai, Negeri Sembilan, Malaysia
[3] Institute of Nanoscience and Nanotechnology, Universiti Putra Malaysia, 43400, Serdang, Selangor, Malaysia

ARTICLE INFO

Article history:
Received 30 April 2024
Received in revised form 25 June 2024
Accepted 8 July 2024
Available online 30 July 2024

Keywords:
Natural source; activated carbon; 3D designs; CST simulation; honeycomb geometry

ABSTRACT

Modern technological advances and developments pose a serious threat to our lives that create more electromagnetic (EM) interference pollution. This situation encourages researchers to produce EM absorbers from various materials. This paper investigates the capability of activated carbon (AC) extracted from *Terminalia catappa* (TC) fruit agricultural waste by the carbonization process as a potential filler for EM absorbers. Besides, AC produced from TC fruit waste also serves plenty of advantages as renewable resources, eco-friendly materials, and exhibits nano-porosity structure. The 3 wt% AC material as a filler is incorporated in the epoxy resin as a polymer matrix using the moulding technique. The sample's EM wave properties are measured using a Vector Network Analyzer (VNA) at a frequency range of 4.0 GHz to 8.0 GHz. The reflection loss (RL) value of AC/epoxy is -8.568 dB at a frequency of 6.68 GHz. To maximize the EM absorption, the geometrical structure of the material is tuned and simulated with different 3D honeycomb designs (1 mm, 2 mm, and 3 mm thickness). The Computer Simulation Technology (CST) simulation predicted and visualized the EM absorption performance of the 3D designs. The CST results of the composite sample exhibited a significant and enhanced effective EM absorption at the C-band frequency range.

1. Introduction

According to numerous research studies, electromagnetic (EM) interference pollution is getting worse today. Mobile phones, Digital Enhanced Cordless Telecommunication (DECT), Bluetooth, base stations, Wi-Fi, 4G, and 5G are the main sources of EM pollution, which is extremely harmful to humans as well as animals. The harmful effects of EM pollution not only have an impact on the physical and biological health of both humans and animals but also the climate and societal behaviour as also reported by Deruelle [1].

* *Corresponding author.*
E-mail address: fadzidahmohdidris@usim.edu.my

https://doi.org/10.37934/aram.122.1.8298

Up until 1st January 2023, an observational study investigated 14 different research findings on the changes in gene expression, oxidant parameters, antioxidant parameters and DNA damage parameters in the umbilical cord blood of the foetus and foetal developmental disorders, cancers, and childhood development disorders involving maternal exposure towards EM fields especially in the first trimester of pregnancy. The biochemical parameters of the umbilical cord blood examined showed high oxidative stress reactions, changes in protein gene expression, DNA damage and increased embryonic abnormalities. Exposure to ionizing and non-ionizing radiation can lead to the enhancement of different cell-based cancers and developmental disorders such as speech problems in childhood as reported by Kashani *et al.,* [2].

The process of EM wave absorption occurs when microwaves hit a material. A portion of the energy is passed through the surface, reflected, and partially absorbed. Dielectric characteristics have been used to describe the portions of energy that fit into these three categories (absorption, reflection, and transmission). Eq. (1) describes the complex relative dielectric constant, ε^* of the material as the fundamental electrical property that describes the interactions.

$$\varepsilon^* = \varepsilon' - j\varepsilon'' \tag{1}$$

where the dielectric constant is denoted by ε' while the dielectric loss is denoted by ε''. In the meantime, Eq. (2) explains the absolute permittivity of a vacuum, ε_0:

$$C_0 \mu_0 \varepsilon_0 = 1 \tag{2}$$

where, C_0 is the speed of light, and μ_0 is magnetic constant. The value for ε_0 and μ_0 are 8.854 x 10^{-12} F/m and 1.26 x 10^{-6} H/m respectively. Materials that do not contain any magnetic components, only react to the electric field as reported by several authors [3], [4]. Moreover, the magnetic and electric fields, which are known to be interrelated, are the two components of electromagnetic waves. An absorbing substance must cancel out the EM wave's strong magnetic or electric field to properly attenuate it. As a result, magnetic and dielectric absorbers can be distinguished among EM wave-absorbing materials as also reported by several research authors [5-7].

The purpose of an EM absorber is to both absorb radiation and create a non-reflective environment, which stops radiation from reflecting. An EM absorber should also have a broad absorption frequency range and be lightweight. Conventional absorbing materials have a high density despite having good absorption capacities, such as ferrite material, and a magnetic absorber. Additionally, as frequency increases, the permeability drastically drops. The advantage of dielectric absorbers is that their density is significantly lower than that of magnetic absorbers. Low-density EM wave absorbing materials are currently receiving attention due to the development of dielectric absorbers such as carbon black, carbon spheres, carbon nanotubes, and porous carbon materials as reported by several authors [5,8,9].

The high consequence of EM pollution has encouraged the development of new nanomaterials with exceptional reflection loss (RL), low thickness, broad bandwidth, and low weight to increase the effectiveness of EM absorption while preserving an easy production method. Technically, microwave absorption is primarily accomplished by EM absorption materials contributed by magnetic loss, dielectric loss, and other mechanisms as reported by an author [10].

Carbon-based nanomaterials have a lot of good qualities such as outstanding dielectric properties which result in good dielectric loss. In addition, the geometrical structure of carbon-based nanomaterials itself helps to improve the EM absorption performance. An EM absorber is lightweight because of the low density of carbon-based nanoparticles. High electrical conductivity in carbon-

based nanomaterials with a high degree of graphitization will increase the imaginary component of the relative complex permittivity, resulting in good dielectric loss properties. This type of material also has good interfacial polarization because of its porosity, high specific surface area and heterogenous structures which indicate a good EM absorbing material as reported by an author [10]. Carbon is also a great semiconductor material that is very suitable for converting microwave energy since microwaves are hampered when they travel through it [11]. Among semiconductors, carbon allows a small amount of charge to pass through it. Carbon attenuates and weakens the microwave signal as it touches it. When energy is lost because of EM interference energy being converted to thermal energy, the cancellation phase will occur [12].

Additionally, activated carbon (AC) has been extensively used in a variety of industrial applications, such as technologies for the purification of gases and the removal of organic pollutants from water. It is also used as an electrode material in electrochemical devices and as a catalyst or catalyst support in catalytic processes [13]. The reason for the wide range of applications is the activated carbon's well-developed pore structure with pore diameters ranging from micro- to macro-pores and a high specific surface area. The dielectric loss brought on by polarisation relaxation can be increased by the porous structure. Also, the solid-void material can enhance the microwave attenuation qualities by multiple microwave reflections and scatterings that allow the wave to dissipate into heat [14,15].

Furthermore, numerous studies and efforts have been made to replace the pricey and non-environmentally friendly absorber material with natural alternatives. Since most of the materials under study are derived from agricultural waste, the natural material is more affordable and ecologically friendly. This research evaluated the efficacy of several types of agricultural waste with commercial absorbers using a range of forms, shapes, and sizes [11]. AC could be produced from various agricultural waste. One of the most common sources of AC is from oil palm waste which is taken from kernels, shells, and empty fruits to adsorb nitric oxide, nitrogen in air and to remove 4-chloro-2-methoxyphenol in aqueous solution[16-18]. AC also can be produced from unique agricultural waste such as sago industrial waste [19], coconut shell [20-23], rice husk [24], used tea leaves [25], honeydew rind [26], coffee waste [27], date seed [28], eggshells [29], rambutan peels [30], sugarcane waste [31] and moringa [32,33].

Moreover, the *Terminalia catappa* (TC) tree has whorled branches, a smooth, grey bark, a fibrous, porous pericarp, and a firm endocarp that encloses the delicious seed are all characteristics of the gigantic deciduous tree. The fruit of the Indian almond tree consists of a husk (34.08%), a kernel (10.32%), a fibrous coating (8.97%), and a hard endocarp (46.63%). A substantial number of fruit shells are wasted as waste agricultural biomass in addition to the normal biological cycle because this tree has various uses for lumber. 89.68% of the fruit's total weight, or the fraction of the fruit that excludes the kernel, is used in the current study as the precursor for making activated carbon as reported by an author [34].

There were many ways to produce AC from TC fruits based on the previous study. One of the methods is by dehydration-carbonization where the AC is immersed in sulphuric acid, H_2SO_4, before the carbonisation process at 600 °C. Another method is the carbonisation process of TC shells followed by the chemical activation using phosphoric acid, H_3PO_4 or three-step process which involves pre-carbonisation, chemical activation using potassium hydroxide, KOH and microwave irradiation [14,35,36].

The geometrical structure of the EM absorber has a significant impact on the EM absorption performance. The honeycomb, a naturally occurring periodic structure (meta-structure) with exceptional absorption properties that are lightweight and sturdy, has been the subject of numerous attempts to be used in the preparation of EM absorbers. As a result of the honeycomb structure's

capacity to optimise convection for heat dissipation, honeycomb microwave absorbers have the advantage due to the mass-to-mechanical strength ratio. The honeycomb microwave absorbers can also handle high power levels that are frequently used in aeroplanes, below spiral antennas, or in anechoic chambers used for high power measurements instead of conventional pyramidal foams [37,38]. In addition, the physical properties of honeycomb structures are low density, high stiffness to weight ratio, high energy absorption, and excellent anti-shock qualities. Honeycomb geometry structure also use minimum quantity of material which can minimize the weight and cost [39].

2. Methodology

2.1 Fabrication of Activated Carbon (AC) from Terminalia catappa (TC) Fruits Agricultural Waste

The *Terminalia catappa* (TC) fruit waste was collected (Malaysian East Coast region) and dried under scorching sun for 48 hours which later were oven-dried for 24 hours at 110 °C as shown in Figure 1 and Figure 2. The exocarp (external shells) and mesocarp (husk) of TC fruits were removed and cleaned to obtain the endocarp of TC fruits as shown in Figure 3. The endocarp parts were ground using high-energy crusher (Grinding Ultra-fine Milling Machine Grains from Min Wang Shanghai, China) until the powder grain size was achieved and sieved the powdered sample using a sieve plate (size: 25 µm). The crushed TC was labelled as TC0 which then went through the milling process using high-energy ball milling (HEBM) method (SPEX SamplePrep 8000D Mixer/Mill®) at a rotational speed of 1200 rpm for 12 hours and the sample was labelled as TC12.

Fig. 1. TC fruit waste collected from the Malaysian East Coast region

Fig. 2. Oven-dried TC fruit waste

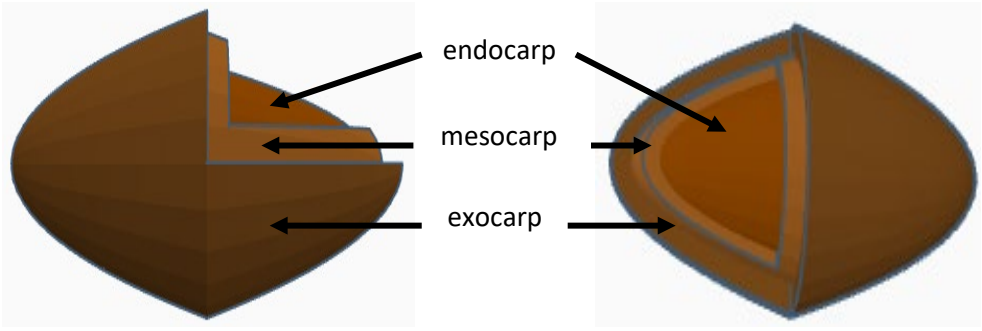

Fig. 3. The schematic structure of TC fruit

Next, both the TC0 and TC12 were pre-carbonized in a ceramic horizontal tube furnace at 400 °C for 4 hours and the samples were chemically activated by impregnation method with 50% potassium hydroxide, KOH (1:5 ratio) at a room temperature for 24 hours. The samples were dried and ground before the carbonization process. The carbonization process of TC0 and TC12 took place in the ceramic horizontal tube furnace at a temperature of 750 °C with a nitrogen flow (5 sccm) for 2 hours to produce the activated carbon samples labelled as AC0 and AC12. Following that, both AC0 and AC12 were washed with distilled water to remove the residues and were washed repeatedly until the washing solution was neutralized (pH 7). The washed AC0 and AC12 were filtered and dried in the oven for 12 hours at 110 °C. The sample labels and their descriptions are summarized in Table 1.

Table 1
Sample labels and description

Sample labels	Material description
TC fruits	Sun and oven-dried, separated and cleaned the endocarp.
TC0	Cleaned endocarps were ground into powder and sieved using a sieve plate size of 25 µm.
TC12	The sieved and crushed TC sample went through the milling process for 12 hours using the high-energy ball milling (HEBM) method.
AC0	AC produced from TC0.
AC12	AC produced from TC12.

2.2 Activated Carbon/Epoxy (AC/Epoxy) Composites

For the preparation of activated carbon/epoxy (AC/epoxy) composite where AC was used as the filler and epoxy resin was used as the polymer matrix. 3 wt.% of both AC of crushed *Terminalia catappa* (TC) powder (AC0) and 12 hours milled TC (AC12) were mixed with the epoxy resin together with the hardener using high energy mixer. Both samples were labelled as AC0/epoxy and AC12/epoxy composites, respectively. The polymer mixtures were poured into the mould with 1 mm thickness and the sample dimensions are as shown in Figure 4.

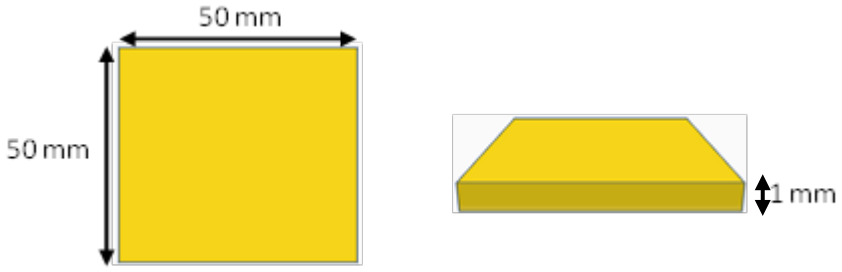

(a) Top view (b) Side view

Fig. 4. Dimensions of AC/epoxy samples from the (a) top view and (b) the side view

2.3 Materials' Characterizations

The particle size of the samples was measured using a Transmission Electron Microscope (TEM) to analyse the pore structure of activated carbon (AC) and *Terminalia catappa* (TC) powder. The

morphology and microstructure analysis of the samples were characterized by Field Emission Scanning Electron Microscope (FESEM) using JSM-IT800 Schottky. Meanwhile, the X-Ray Diffraction (XRD) method used for phase analyses was examined using Rigaku MiniFlex 600. The microwave absorption performance for each AC polymer composite (AC0/epoxy and AC12/epoxy) was determined using a Vector Network Analyzer (VNA) using Agilent PNA N5227A at a frequency range of 4.0 GHz to 8.0 GHz (C-band).

2.4 Computer Simulation and 3D Designs

The 3D honeycomb structures were designed and the microwave absorptions for C-band (4.0 GHz to 8.0 GHz) were simulated using CST Studio Suite based on the obtained dielectric and magnetic results (permittivity, ε and permeability, μ) from the Vector Network Analyser (VNA) data. The honeycomb (hexagon) unit cell has a different range of radius, a (a= 1 mm, 2 mm, and 3 mm) and a different range of thickness (1 mm, 2 mm, and 3 mm), with the total of b (0.6 mm, 1.6 mm, 2.6 mm) and base of 0.4 mm as shown and listed in Figure 5 and Table 2, respectively. Figure 6 shows the honeycomb unit cell with respective dimensions that were arranged in a series of honeycomb structures and cut to fit the C-band waveguide before the simulation.

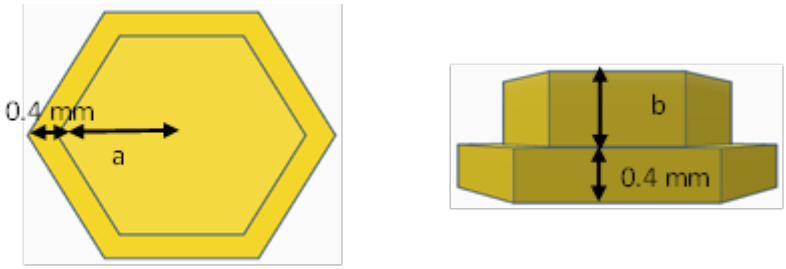

(a) Top view (b) Side view

Fig. 5. Honeycomb unit cell from the (a) top view and (b) side view

Table 2
Dimensions of honeycomb unit cell

Radius, a (mm)	Label	Thickness (mm)	Label	Sample labels
1	1	1	A	A1
2	2			A2
3	3			A3
1	1	2	B	B1
2	2			B2
3	3			B3
1	1	3	C	C1
2	2			C2
3	3			C3

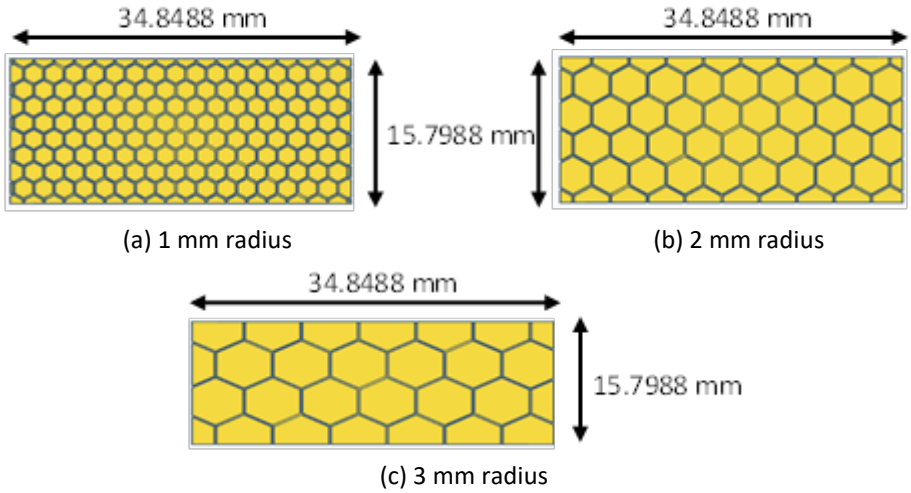

(a) 1 mm radius (b) 2 mm radius

(c) 3 mm radius

Fig. 6. Honeycomb series of (a) 1 mm (b) 2 mm and (c) 3 mm radius, a, and each with the C-band waveguide size

Since there were so many unit cells in the simulation, the time domain solver was employed. The time domain solver was used for the simulation due to the high number of unit cells. The frequency domain solver is particularly slow and memory heavy if the number of mesh cells is enormous since it involves the solution of a matrix equation for exceptionally large structures or frequencies. The time domain solution ought to be the best option given the vast number of cells. The S_{11} and S_{21} of the absorber are carried out, hence the reflectance, R and transmittance, T can be calculated as shown in Eq. (3) and Eq. (4) respectively [40,41]:

$$R = |S_{11}|^2 \tag{3}$$

$$T = |S_{21}|^2 \tag{4}$$

Due to the metal backplane, T = 0, and the absorption rate, A can be calculated as in Eq. (5) [40,41]:

$$A = 1 - R = 1 - |S_{11}|^2 \tag{5}$$

3. Results and Discussion

3.1 Particle Size Analysis

Figure 7 shows the micrograph of *Terminalia catappa* (TC) milled for 12 hours (TC12) measured by using a Transmission Electron Microscope (TEM). The average particle size of the TC12 is ~51.8 nm. The particle size decreases due to the milling process. As the milling time increases, the particles reduce to smaller particle sizes. However, there are particles which are agglomerated although the powder was dispersed in an ethanol solution during sample preparation for measurement.

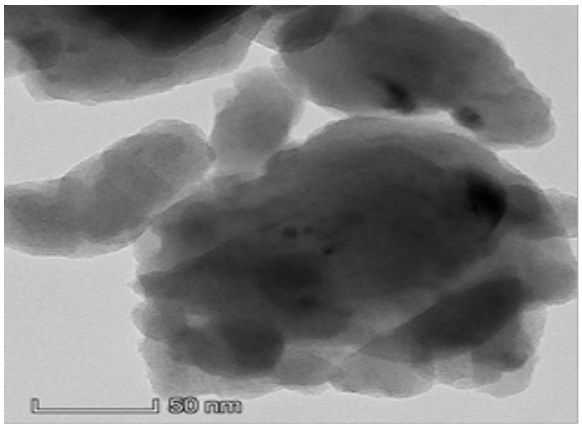

Fig. 7. In TEM micrograph of TC12

3.2 Microstructural Analysis

Field Emission Scanning Electron Microscopy (FESEM) analysis was done to study the morphological structure of the synthesised activated carbon. Figure 8 shows FESEM images of a) *Terminalia catappa* (TC) powder milled for 12 hours (TC12) and b) activated carbon (AC) produced from 12 hours of mill TC powder (AC12) at a magnification of 10,000 and 1,000 respectively. Mehmandost *et al.,* [42] reported that the surface of TC is dense and rough. It could also be observed that TC has no pores (non-porous) and no voids.

On the other hand, the activated carbon has an average pore size of 62 nm. The surface of activated carbon grains has a porous microstructure, with open large macropores (in microns) between grains of varying sizes and randomly distributed throughout the sample. The formation of porous structure also results from the pre-carbonization process and activation process by using potassium hydroxide, KOH as an activating agent. The formation of an irregular porous structure creates more transmission routes that enhance the multiple reflections in the structure. The pores structure also may contribute to a better match between dielectric loss and magnetic loss.

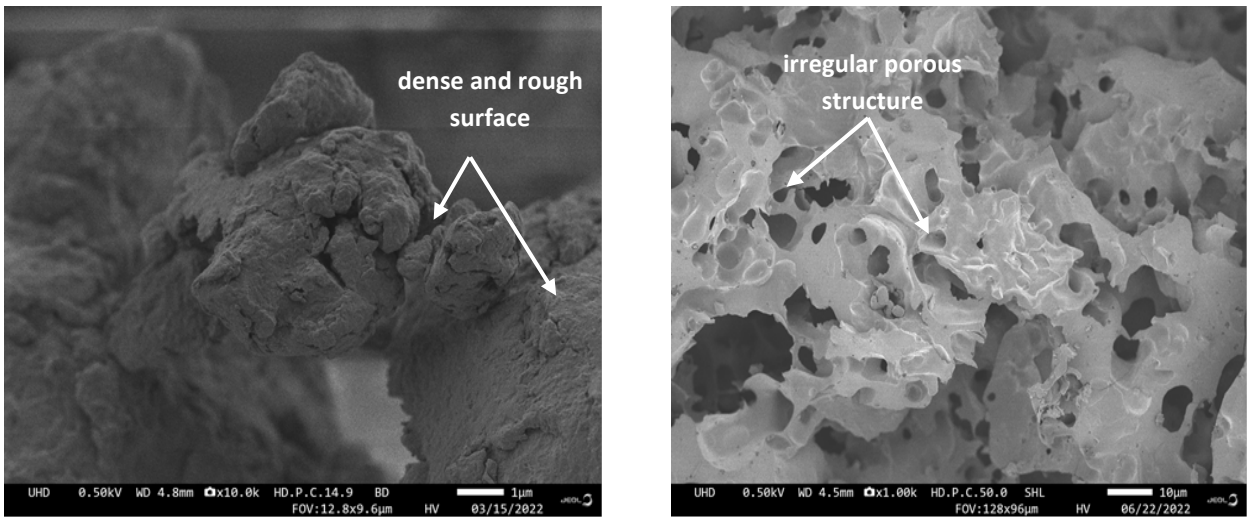

(a) TC12 (b) AC12

Fig. 8. FESEM images of (a) TC12 and (b) AC12

3.3 Phase Analysis

The phase analysis of *Terminalia catappa* (TC) and activated carbon (AC) was carried out by using an X-Ray Diffractometer (XRD) at the 2θ angle between 10^0 to 90^0. Figure 9 shows the X-ray diffraction pattern of TC milled for 12 hours (TC12) and activated carbon of 12 hours milled TC (AC12) from TC powder. The diffraction patterns of AC were matched with the standard ICDD data (00-001-0646). The presence of a broad peak at 2θ around 21^0 confirms the presence of porous and amorphous structures. The obtained diffraction peaks of (002), (100) and (101) crystal planes correspond to graphitic carbon that reflects the turbostratic carbon structure.

The crystallite size can be measured by using Scherrer Eq. (6):

$$D = \frac{(0.89\lambda)}{(\beta \cos\theta)} \tag{6}$$

where *D* is the crystallite size, 0.89 is the Debye constant, λ is the wavelength of the X-ray used, θ is Bragg's angle and β is the full-width half maximum (FWHM) as reported by an author [43].

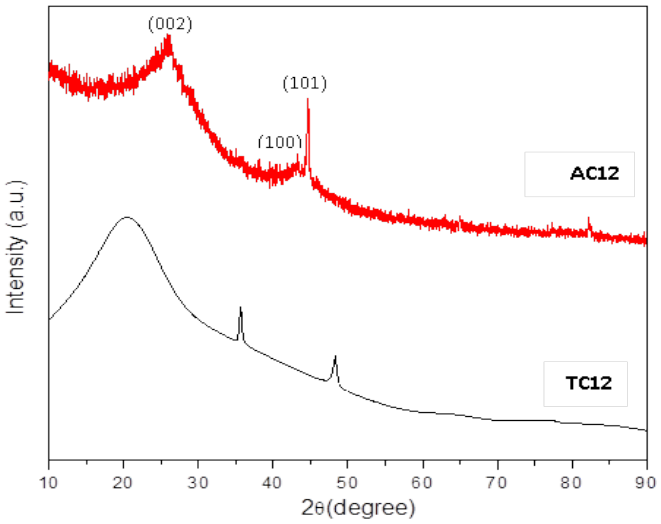

Fig. 9. XRD pattern of TC12 and AC12 from TC powder

It is calculated from the full width at half maximum (FWHM) value of the high-intensity peak corresponding to the (101) crystal plane of AC. Table 3 shows the angle 2θ (^{0}), d spacing (Å), intensity (cts), FWHM (2θ), and crystallite size (nm) of TC 12 and AC 12. The average crystallite size for TC 12 and AC 12 are 14.7 nm and 30.7 nm respectively. On the other hand, the value of d spacing between 2.0 and 2.5 refers to the distance between parallel planes of atoms used to construct molecular nanostructures, resulting in intraparticle microporous nanostructures of various shapes and sizes.

Table 3
XRD data

Sample	2θ (^{0})	d spacing (Å)	Intensity (cts)	FWHM (2θ)	Crystallite size (nm)
TC12	35.5308	2.52457	129.27	0.5760	14.7
AC12	44.5713	2.03125	261.80	0.2880	30.7

3.4 Microwave Characterisation

The dielectric and magnetic properties of activated carbon/epoxy (AC/epoxy) composites for both AC obtained from crushed *Terminalia catappa* (TC) powder (AC0), and AC produced from 12 hours milled TC (AC12) in C-band frequency range were determined using Vector Network Analyser (VNA) as shown in Figure 10.

According to Debye's theory, interfacial polarisation of the electrons and dipolar polarisation are connected to the real permittivity, ε'. The imaginary permittivity, ε" is associated with dielectric loss. The lossless and lossy responses of the material are represented by the real permeability, μ' and the imaginary permeability, μ'' components, respectively as reported by several authors [44], [45]. Also, the parameters of the relative complex permittivity, ε_r in Eq. (7) and the relative complex permeability, μ_r in Eq. (8) are connected to the absorptivity of absorbers as shown in the equations below:

$$\varepsilon_r = \varepsilon' - i\varepsilon" \tag{7}$$

$$\mu_r = \mu' - j\mu" \tag{8}$$

where real (ε' and μ') and imaginary (ε" and μ") parts of both permittivity and permeability equations are related to energy storage capacity and energy dissipation, respectively as reported by an author [46].

The real permittivity, ε' value for both AC0 and AC12 are constant along the 4.0 GHz to 8.0 GHz with the value of 6.100 and 7.011 respectively. In contrast to the real permittivity, ε', there are fluctuations in the imaginary permittivity, ε" of AC0. Figure 10(a) shows the increment from 0.513 to 0.621 at the frequency of 4.0 GHz to 4.9 GHz and the decrement from 0.621 to the lowest peak value of 0.232 at 4.92 GHz to 7.02 GHz. The values of imaginary permittivity, ε" of AC0 were then increased to 0.559 at 8.0 GHz. Furthermore, imaginary permittivity, ε" of AC12 gradually decreased from 1.355 to 0.678 throughout the frequency range.

The real permeability, μ' for AC0 was constant with the value of 3, while the real permeability, μ' of AC12 has minor fluctuations with a value between 3.1 and 3.2 throughout the frequency range of 4.0 GHz to 8.0 GHz. Besides, there were fluctuations in the imaginary permeability, μ" value of AC0 with the lowest value of 1.26 at 4.86 GHz and highest value of 2.031 at 7.46 GHz as shown in Figure 10(a). Based on Figure 10(b), the imaginary permeability, μ" value of AC12 with a gradual increment from 0.440 to 0.951 throughout the frequency range.

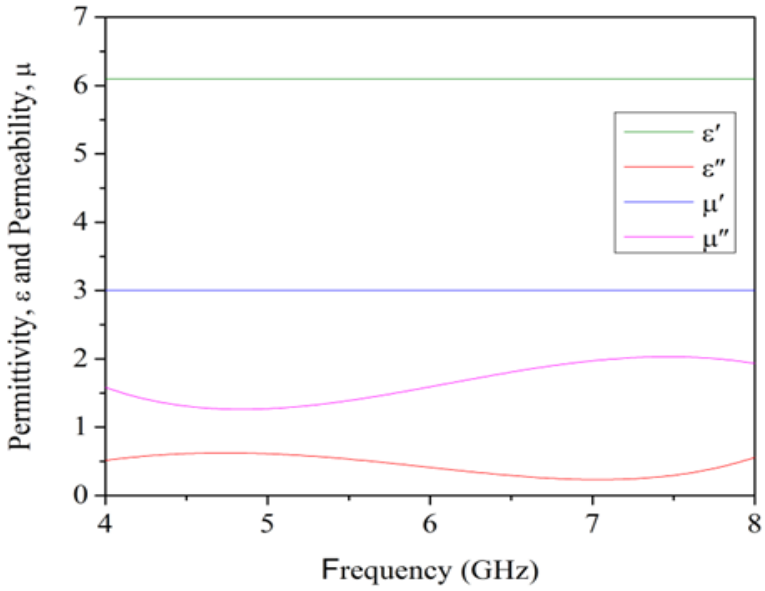

(a) AC0

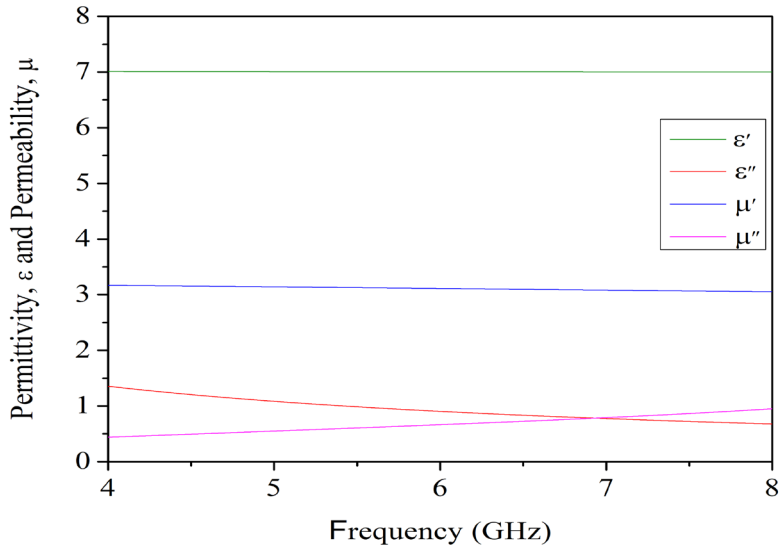

(b) AC12

Fig. 10. The dielectric permittivity, ε (real permittivity, ε' and imaginary permittivity, ε") and the magnetic permeability, μ (real permeability, μ' and imaginary permeability, μ") values of (a) AC0 and (b) AC12

Generally, an EM wave can be reflected, absorbed, or transmitted when it hits a material's surface. Since there is no EM wave transmission during a single port VNA test, the EM wave will only be affected by the material's EM wave reflection and absorption. The ratio of the reflected to incident EM wave power (S_{11} parameter), is the sole scattering parameter that can be determined from a single port VNA measurement. High absorption of EM wave indicates low EM wave reflection of the material. S_{11} parameter is also denoted as reflection loss (RL) as also reported by an author [15].

Next, the RL value of the EM absorber material is used to determine the absorption properties [44]. Duan *et al.,* [47] explained that the RL value can be computed from the relative complex permeability and permittivity using the transmission-line theory and the metal back-panel model in Eq. (9) and Eq. (10):

$$RL\ (dB) = 20\log_{10}\left|\frac{(Z_{in}-1)}{(Z_{in}+1)}\right| \quad (9)$$

$$Z_{in} = \sqrt{\frac{\mu_r}{\varepsilon_r}}\tan h\left(\frac{j2\pi\sqrt{\mu\varepsilon}fd}{c}\right) \quad (10)$$

where Z_{in} is the normalized input impedance. Meanwhile, $\tan h$ is the hyperbolic tangent function, d is the thickness of the material, the microwave frequency is denoted as f and lastly, c represents the speed of light in a vacuum condition. The effective absorption bandwidth (EAB) is the frequency range with the RL value of -10 dB representing more than 90% of the EM waves were absorbed as also reported by an author [47]. Minimum RL value also refers to the highest EM wave absorption and lower return loss.

Figure 11 shows the RL value of AC0 and AC12 polymer composites. The RL value of AC12 is lower than the RL value of AC0 which are -8.568 dB at 6.68 GHz and -5.115 dB at 6.48 GHz respectively. The minimum RL peaks for AC0 and AC12 are both on the same frequency ranges which are ~6.0 GHz to ~7.5 GHz. The minimum RL value of AC0 and AC12 was higher than -10 dB, which indicates the EM absorption for both samples does not exceed the 90% effective absorption. However, the microwave absorption performance could be improved by tuning the geometrical structure of the sample (honeycomb).

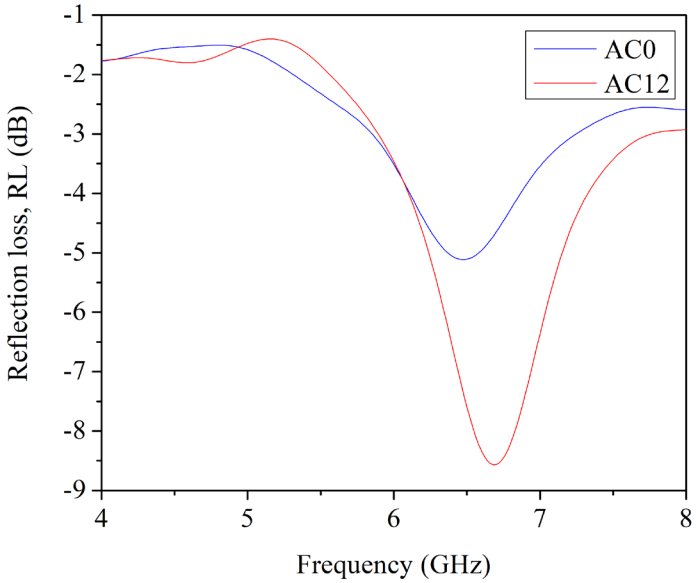

Fig. 11. RL value of AC12 and AC0

3.5 Microwave Simulation

The microwave performance of the honeycomb geometry structure of activated carbon (AC) of 12 hours milled *Terminalia catappa* (TC) powder (AC12) was simulated via CST Studio Suite. The dielectric and magnetic (permittivity, ε and permeability, μ) values of AC12/epoxy composite as the input data were obtained from the experimental microwave absorption by using Vector Network Analyser (VNA).

Figure 12 shows the reflection loss (RL) of honeycomb AC12 with a constant thickness of 1 mm and three different radiuses of honeycomb unit cell (A1= 1 mm thickness and 1 mm radius, A2= 1 mm thickness and 2 mm radius, and A3= 1 mm thickness and 3 mm radius). There was a lot of improvement in terms of electromagnetic (EM) absorption for the samples with honeycomb geometrical structure as the minimum RL value < -10 dB which indicates 90% of EM absorption compared to the original flat design in Figure 11. This is because the honeycomb structure caused

multiple reflections between the honeycomb surface which eventually improves the attenuation of EM as reported by an author [18]. The minimum RL peaks for the honeycomb geometry in Figure 12 are also broader in the range of ~5.0 GHz to ~7.5 GHz and were slightly higher compared to the original design (flat) in Figure 11 where the minimum RL peaks only in the range of ~6.0 GHz to ~7.5 GHz.

Moreover, the RL value decreases as the radius decreases. The minimum RL values for AC12 A1, AC12 A2 and AC12 A3 are -43.978 dB at 6.72 GHz, -43.074 dB at 6.69 GHz and -41.89329 dB at 6.68 GHz respectively. The minimum RL decreases as the radius of the honeycomb decreases due to the increasing amount of honeycomb unit cells that caused the multiple reflections to increase, and this situation enhanced the EM absorption performance. From the minimum RL value in Figure 12, as the radius of the honeycomb unit increases, there is a slight peak shift towards the lower frequency range.

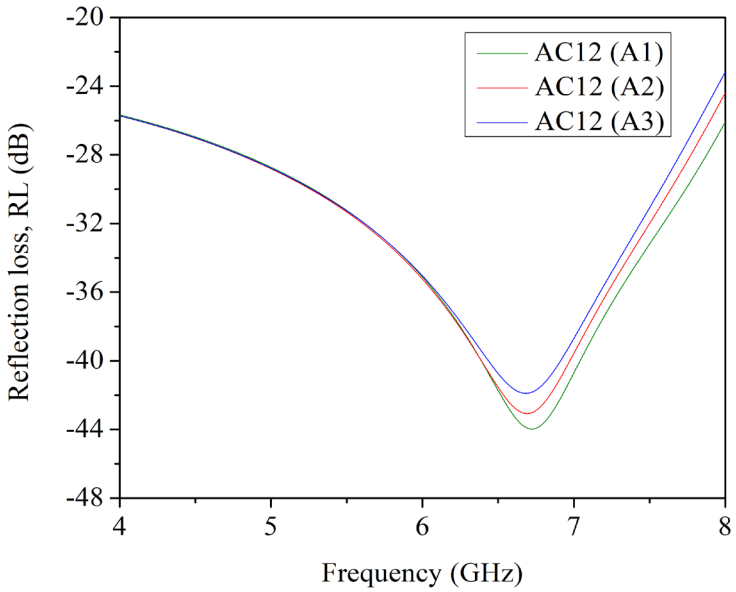

Fig. 12. RL value of honeycomb geometrical structure of AC12 with 1 mm thickness and three different radiuses (1 mm, 2mm and 3 mm)

Further investigation is to determine the relationship between the thickness of the honeycomb geometrical structure and the minimum RL value. Since the RL value of 1 mm radius is the lowest (Figure 12), the microwave simulation of different thicknesses (A1= 1 mm thickness, B1= 2 mm thickness and C1= 3 mm thickness) of honeycomb with a constant radius (1 mm) were simulated and the resulted in RL value as shown in Figure 13.

The minimum RL values of AC12 A1, AC12 B1 and AC12 C1 are -43.97812 dB at 6.72 GHz, -31.10303 dB at 6.08 GHz and -53.80251 dB at 5.82 GHz respectively. Based on the results in Figure 13, the frequency of the minimum RL value decreases as the thickness of the honeycomb increases which results in a peak shift towards a lower frequency range. In the previous studies [19,20], the minimum RL peaks shift toward a lower frequency range as the thickness increases.

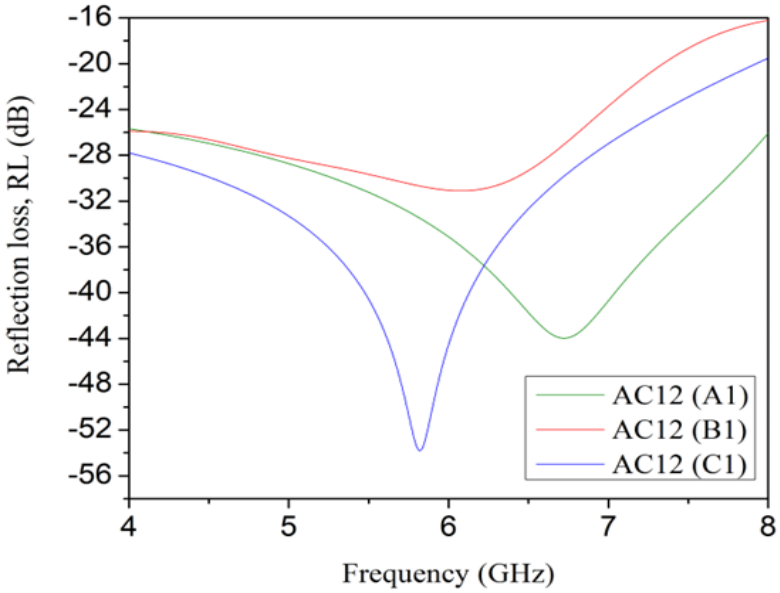

Fig. 13. RL value of honeycomb geometrical structure of AC12 with 1 mm radius and three different thicknesses (1 mm, 2mm and 3 mm)

4. Conclusions

The activated carbon (AC) samples were successfully produced from *Terminalia catappa* (TC) by carbonisation and chemical activation methods with two varied sizes of the starting materials (12 hours milled TC and crushed TC). Based on the particle size, the average particle size of TC milled for 12 hours (TC12) is ~51.8 nm. Meanwhile, morphological structure analysis of TC12 shows a rough surface and no pores. Contrary to AC produced from 12-hour mill TC powder (AC12) with the average pore size of AC12 is 62 nm and a porous microstructure due to carbonization and chemical activation. The phase analysis with a broad peak confirms the presence of porous and amorphous structure in AC12. The reflection loss (RL) results shows both AC obtained from crushed TC powder (AC0) and AC12 composites higher than -10 dB that indicates the electromagnetic (EM) wave absorption for both samples do not exceed the 90% effective absorption. However, the RL results improved the geometrical structure of the samples (honeycomb). The RL results for the honeycomb geometrical structure simulation of AC12 show the minimum RL value < -10 dB and the RL value decreasing as the radius decreases. The frequency of the minimum RL value also decreases as the thickness of the honeycomb increases which results in a peak shift towards a lower frequency range.

For future research, it is recommended to 3D-print the suggested geometry or other geometries to study accurate comparison between the experimental results from the VNA and the computer simulation results using AC produced from TC fruit waste as the filler. The frequency range of EM absorption should be below or higher than the C-band frequency range to further explore the suitable application of AC produced from TC fruit waste as an EM wave absorber.

Acknowledgement
This research was funded by the Ministry of Higher Education (MOHE) of Malaysia under the Fundamental Research Grant Scheme (FRGS/1/2020/STG05/USIM/02/3) (USIM/FRGS/KGI/KPT/52020). This research also acknowledges Institute of Nanoscience and Nanotechnology, Universiti Putra Malaysia for the computer simulation service (CST Studio Suite 2022).

References

[1] Deruelle, Fabien. "The different sources of electromagnetic fields: Dangers are not limited to physical health." *Electromagnetic biology and medicine* 39, no. 2 (2020): 166-175. https://doi.org/10.1080/15368378.2020.1737811

[2] Kashani, Zahra Atarodi, Reza Pakzad, Farzaneh Rashidi Fakari, Mohammad Sadegh Haghparast, Fatemeh Abdi, Zohreh Kiani, Afsaneh Talebi, and Somaieh Moradi Haghgoo. "Electromagnetic fields exposure on fetal and childhood abnormalities: Systematic review and meta-analysis." *Open Medicine* 18, no. 1 (2023): 20230697. https://doi.org/10.1515/med-2023-0697

[3] Venkatesh, M. S., and G. S. V. Raghavan. "An overview of microwave processing and dielectric properties of agri-food materials." *Biosystems engineering* 88, no. 1 (2004): 1-18. https://doi.org/10.1016/j.biosystemseng.2004.01.007

[4] Venkatesh, M. S., and G. S. V. Raghavan. "An overview of dielectric properties measuring techniques." *Canadian biosystems engineering* 47, no. 7 (2005): 15-30.

[5] Chen, Jiabin, Xiaohui Liang, Jing Zheng, Weihua Gu, Chunchuan Pei, Feiyue Fan, and Guangbin Ji. "Modulating dielectric loss of mesoporous carbon fibers with radar cross section reduction performance via computer simulation technology." *Inorganic Chemistry Frontiers* 8, no. 3 (2021): 758-765. https://doi.org/10.1039/D0QI01237H

[6] Wang, Gehuan, Samuel Jun Hoong Ong, Yue Zhao, Zhichuan J. Xu, and Guangbin Ji. "Integrated multifunctional macrostructures for electromagnetic wave absorption and shielding." *Journal of Materials Chemistry A* 8, no. 46 (2020): 24368-24387. https://doi.org/10.1039/D0TA08515D

[7] Zhang, Tao, Sifan Zeng, Guangwu Wen, and Jiaqi Yang. "Novel carbon nanofibers build boron carbonitride porous architectures with microwave absorption properties." *Microporous and Mesoporous Materials* 211 (2015): 142-146. https://doi.org/10.1016/j.micromeso.2015.02.003

[8] Zhou, Ming, Weihua Gu, Gehuan Wang, Jing Zheng, Chunchuan Pei, Feiyue Fan, and Guangbin Ji. "Sustainable wood-based composites for microwave absorption and electromagnetic interference shielding." *Journal of Materials Chemistry A* 8, no. 46 (2020): 24267-24283. https://doi.org/10.1039/D0TA08372K

[9] Li, Ya, Xiaofang Liu, Xiaoyu Nie, Wenwen Yang, Yidong Wang, Ronghai Yu, and Jianglan Shui. "Multifunctional organic–inorganic hybrid aerogel for self-cleaning, heat-insulating, and highly efficient microwave absorbing material." *Advanced Functional Materials* 29, no. 10 (2019): 1807624. https://doi.org/10.1002/adfm.201807624

[10] Zeng, Xiaojun, Xiaoyu Cheng, Ronghai Yu, and Galen D. Stucky. "Electromagnetic microwave absorption theory and recent achievements in microwave absorbers." *Carbon* 168 (2020): 606-623. https://doi.org/10.1016/j.carbon.2020.07.028

[11] Awang Damit, Dayang Suhaida, Mohd Hussaini Abbas, and Hj Hasnain Abdullah. "Preliminary findings of raw bamboo curtain absorber (BCA), charred and coated bamboo ash painted characteristics for electromagnetic wave absorption." *ESTEEM Academic Journal* 13 (2017): 82-91.

[12] M. I. Fazin, A. R. Razali, H. Abdullah@Idris, M. N. Taib, N. Mohd Noor, and N. Mohamad Kassim. 2021. "Electromagnetic Wave Absorption Properties Based on Slot Size of Biomass Hollow Pyramidal Microwave Absorber," Journal of Electrical & Electronic Systems Research, vol. 19, no. OCT2021, pp. 88–94. DOI: 10.24191/jeesr.v19i1.012. https://doi.org/10.24191/jeesr.v19i1.012

[13] Li, Wei, Li-bo Zhang, Jin-hui Peng, Ning Li, and Xue-yun Zhu. "Preparation of high surface area activated carbons from tobacco stems with K2CO3 activation using microwave radiation." *Industrial crops and products* 27, no. 3 (2008): 341-347. https://doi.org/10.1016/j.indcrop.2007.11.011

[14] Awitdrus, Awitdrus. "Preparation of Terminalia catappa Shell Based Activated Carbon by Microwave Assisted Chemical Activation." *Journal of Technomaterials Physics* 1, no. 1. (2019). https://doi.org/10.32734/jotp.v1i1.820

[15] Chitraningrum, Nidya, Resti Marlina, Ria Yolanda Arundina, Ester Rimma Suryani Togatorop, Sulistyaningsih Sulistyaningsih, Hana Arisesa, Ismail Budiman, Pamungkas Daud, and Mohammad Hamzah. "Microwave absorption properties of porous activated carbon-based palm oil empty fruit bunch." *AIP Advances* 12, no. 11 (2022). https://doi.org/10.1063/5.0128960

[16] Ahmada, M. A., W. M. A. W. Dauda, and M. K. Arouab. "CARBON MOLECULAR SIEVES FROM CARBON DEPOSITION OVER PALM SHELL BASED ACTIVATED CARBON." *Solid State Science and Technology* 15, no. 1 (2007): 127–134.

[17] Hamad, Bakhtiar K., Ahmad Md Noor, and Afidah A. Rahim. "Removal of 4-chloro-2-methoxyphenol from aqueous solution by adsorption to oil palm shell activated carbon activated with K2CO3." *Journal of physical science* 22, no. 1 (2011): 39-55.

[18] Lin, Cha Soon, Naimah Ibrahim, Norhidayah Ahmad, Muhammad Adli Hanif, and Sureena Abdullah. "Nitric oxide removal by zinc chloride activated oil palm empty fruit bunch fibre." *Malaysian J Fundam Appl Sci* 17 (2021): 84-89. https://doi.org/10.11113/mjfas.v17n1.2171

[19] Makshut, Nur Aqilah, Zainab Ngaini, Rafeah Wahi, Hasnain Hussain, Nurul Iwani Mahmut, and Nurul Qhalila Bahrin. "Nano-Sized Adsorbent from Pyrolysed Sago Activated Sludge for Removal of Pb (II) from Aqueous Solution." *Pertanika Journal of Science & Technology* 28, no. 3 (2020): 893–916.

[20] Adnan, Raudah Mohd, Thayabharan Yanasergaran, Dilaeleyana Abu Bakar Sidik, Nur Shahirah Mohd Aripen, Hafsa Mohammad Noor, Adnin Afifi Nawi, and Darsshan Raman. "Performance of Coconut-shell Activated Carbon on Methylene Blue Treatment." *International Journal of Business and Technology Management* 5, no. S5 (2023): 218-224. https://doi.org/10.55057/ijbtm.2023.5.S5.24

[21] Abd Rashid, Ramlah, Mohd Azlan Mohd Ishak, and Kasim Mohammed Hello. "Adsorptive removal of methylene blue by commercial coconut shell activated carbon." *Science Letters (ScL)* 12, no. 1 (2018): 77-101.

[22] Amran, Fadina, Nur Fatiah Zainuddin, and Muhammad Abbas Ahmad Zaini. "Two-stage adsorber design for methylene blue removal by coconut shell activated carbon." *Malaysian Journal of Fundamental and Applied Sciences* 17, no. 6 (2021): 768-775. https://doi.org/10.11113/mjfas.v17n6.2303

[23] Anuar, Muhammad'Azib Khairul, Noor Sabariah Mahat, Nurfarhain Mohamed Rusli, Muhd Nazrul Hisham Zainal Alam, and Muhammad Abbas Ahmad Zaini. "Insight into the optimization of mass and contact time in two-stage adsorber design for malachite green removal by coconut shell activated carbon." *International Journal of Biomass and Renewables* 10, no. 2 (2021): 1-8. https://doi.org/10.61762/ijbrvol10iss2art12871

[24] Collin, JOSEPH G., and F. R. A. N. K. I. E. Yii. "Textural and chemical characterisation of activated carbons prepared from rice husk (Oryza sativa) using a two-stage activation process." *Journal of Engineering Science and Technology* 3, no. 3 (2008): 234-242.

[25] Menon, R., J. Singh, V. Doshi, and Xiao Y. Lim. "Investigation on spent tea leaves derived activated carbon for co 2 adsorption." *J Eng Sci Technol EURECA* (2014): 50-61.

[26] Yunus, Zalilah Murni, Norzila Othman, Rafidah Hamdan, and Nurun Najwa Ruslan. "Honeydew Rind Activated Carbon as an Adsorbent for Zn (II) and Cr (III) Removal from Aqueous Solution: An Optimization Study." *Pertanika Journal of Science & Technology* 25, no. 105 (2017): 155-162.

[27] Chaiw, Yong Ni, Keat Ki Ang, Ting Lee, and Xiao Y. Lim. "Investigation of the coffee waste-derived adsorbent." *J. Eng. Sci. Technol* 2 (2016): 16.

[28] Ghazali, S. A., and Jamil Mohamed Sapari. "Preparation of date seed activation for surfactant recovery." *Malaysian Journal of Analytical Sciences* 21, no. 5 (2017): 1045-1053. https://doi.org/10.17576/mjas-2017-2105-06

[29] Habeeb, Omar Abed, Ramesh Kanthasamy, Gomaa Abdelgawad Mohammed Ali, and Rosli Mohd Yunus. "Model isoterma berdasarkan kajian penjerapan hidrogen sulfida terlarut daripada air sisa menggunakan karbon yang diaktifkan berasaskan kulit telur." *Malaysian Journal of Analytical Sciences* 21, no. 2 (2017): 334-345. https://doi.org/10.17576/mjas-2017-2102-08

[30] Aziz, A. Z. R. I. N. A., Mohamad Firdaus Mohamad Yusop, and Mohd Azmier Ahmad. "Removal of bisphenol S from aqueous solution using activated carbon derived from rambutan peel via microwave irradiation technique." *Sains Malays* 51, no. 12 (2022): 3967-3980. https://doi.org/10.17576/jsm-2022-5112-08

[31] Musa, Mutah, Akira Kikuchi, Zaiton Abdul Majid, Jafariah Jaafar, and Mohd Salim. "Activated carbon production from agricultural biomass using response surface method (RSM) for Cd (II) removal." *Jurnal Teknologi (Sciences and Engineering)* 69, no. 3 (2014): 59-64. https://doi.org/10.11113/jt.v69.3144

[32] Alias, Nurul Zawani, Noor Aina Mohamad Zuki, Siti Hajar Alias, and Mohd Lias Kamal. "Removal of iron (Fe) by adsorption using activated carbon moringa oleifera (ACMO) in aqueous solution." *Jurnal Intelek* 7, no. 2 (2012): 22-29.

[33] Azad, Md Shahin, Syaza Azhari, and Mohd Sukri Hassan. "Removal of Methylene blue, Escherichia coli and Pseudomonus aeruginosa by Adsorption Process of Activated Carbon Produced from Moringa oleifera Bark." *Malaysian Journal of Science Health & Technology* 7 (2020). https://doi.org/10.33102/mjosht.v7io.105

[34] Harborne, Jeffrey B. "The wealth of India, raw materials, volume 1a, revised edition: produced and published by the Publications and Information Directorate, CSIR, Hillside Road, New Delhi, 110012, 1985. 512 pp. $47." *Phytochemistry* 26, no. 9 (1987): 2654-2654. https://doi.org/10.1016/S0031-9422(00)83907-2

[35] Aldila, Herman, Megiyo Megiyo, Fitri Afriani, and Yuant Tiandho. "ANALYSIS OF INFLUENCE OF ACTIVATOR CONCENTRATION ON CHARACTERISTICS OF ACTIVATED CARBON FROM KETAPANG SHELL (Terminalia Catappa) BASED ON IMAGE PROCESSING METHOD." *Jurnal Geliga Sains: Jurnal Pendidikan Fisika* 6, no. 1 (2018): 1-8. https://doi.org/10.31258/jgs.6.1.1-8

[36] Hassan, L. G., A. Uba, S. W. Hassan, S. Yusuf, M. A. Sokoto, and A. N. Itodo. "Evaluation of Biological Oxygen Demand (BOD) and Chemical Oxygen Demand (COD) Removal from Tannery Wastewater using Activated Carbon from Terminalia catappaNutshells." (2018). https://doi.org/10.47469/JEES.2018.v06.100065

[37] Zhou, Qian, Chenxi Qi, Tiantian Shi, Yuekun Li, Wei Ren, Shengyue Gu, Bei Xue, Fang Ye, Xiaomeng Fan, and Lifei Du. "3D printed carbon based all-dielectric honeycomb metastructure for thin and broadband electromagnetic

absorption." *Composites Part A: Applied Science and Manufacturing* 169 (2023): 107541. https://doi.org/10.1016/j.compositesa.2023.107541

[38] Laur, Vincent, Azar Maalouf, Alexis Chevalier, and Fabrice Comblet. "Three-dimensional printing of honeycomb microwave absorbers: Feasibility and innovative multiscale topologies." *IEEE Transactions on Electromagnetic Compatibility* 63, no. 2 (2020): 390-397. https://doi.org/10.1109/TEMC.2020.3006328

[39] Ansari, Z., C. W. Tan, M. R. M. Rejab, D. Bachtiar, J. Siregar, M. Y. M. Zuhri, and N. S. D. M. Marzuki. "Crushing behaviour of composite square honeycomb structure: a finite element analysis." *Journal of Mechanical Engineering and Sciences* 11, no. 2 (2017): 2637-2649. https://doi.org/10.15282/jmes.11.2.2017.7.0241

[40] Li, Si-Jia, Peng-Xin Wu, He-Xiu Xu, Yu-Long Zhou, Xiang-Yu Cao, Jiang-Feng Han, Chen Zhang, Huan-Huan Yang, and Zhao Zhang. "Ultra-wideband and polarization-insensitive perfect absorber using multilayer metamaterials, lumped resistors, and strong coupling effects." *Nanoscale research letters* 13 (2018): 1-13. https://doi.org/10.1186/s11671-018-2810-0

[41] Al-badri, Khalid Saeed Lateef, Yadgar I. Abdulkarim, Fatih Özkan Alkurt, and Muharrem Karaaslan. "Simulated and experimental verification of the microwave dual-band metamaterial perfect absorber based on square patch with a 450 diagonal slot structure." *Journal of Electromagnetic Waves and Applications* 35, no. 11 (2021): 1541-1552. https://doi.org/10.1080/09205071.2021.1905560

[42] Mehmandost, Nasrin, Nasser Goudarzi, Mansour Arab Chamjangali, and Ghadamali Bagherian. "Removal of methylene blue and crystal violet in binary aqueous solution by magnetic Terminalia catappa kernel shell biosorbent using Box–Behnken design." *Journal of the Iranian Chemical Society* 19, no. 9 (2022): 3769-3781. https://doi.org/10.1007/s13738-022-02552-5

[43] Anandhi, S., A. Sagaya Amala Immanuel, V. Ramkumar, and C. Sudhakar. "Effect of solvent on ZnO nanoparticles by simple sol-gel method." *Materials Today: Proceedings* (2023).

[44] Yu, Zhaoju, Xuan Lv, Kangwei Mao, Yujing Yang, and Anhua Liu. "Role of in-situ formed free carbon on electromagnetic absorption properties of polymer-derived SiC ceramics." *Journal of Advanced Ceramics* 9 (2020): 617-628. https://doi.org/10.1007/s40145-020-0401-x

[45] Jadav, Mudra, and S. P. Bhatnagar. "Particle size controlled magnetic loss in magnetite nanoparticles in RF-microwave region." *IEEE Transactions on Magnetics* 56, no. 7 (2020): 1-8. https://doi.org/10.1109/TMAG.2020.2990769

[46] Chen, Honghui, Wenle Ma, Zhiyu Huang, Yi Zhang, Yi Huang, and Yongsheng Chen. "Graphene-based materials toward microwave and terahertz absorbing stealth technologies." *Advanced Optical Materials* 7, no. 8 (2019): 1801318. https://doi.org/10.1002/adom.201801318

[47] Duan, Wenyan, Xiaowei Yin, Quan Li, Lorenz Schlier, Peter Greil, and Nahum Travitzky. "A review of absorption properties in silicon-based polymer derived ceramics." *Journal of the European Ceramic Society* 36, no. 15 (2016): 3681-3689. https://doi.org/10.1016/j.jeurceramsoc.2016.02.002